Semaphorin 7a Links Nerve Regeneration and Inflammation in the Cornea

Abed Namavari, Shweta Chaudhary, Okan Ozturk, Jin-Hong Chang, Lisette Yco, Snehal Sonawane, Neelima Katam, Vishakha Khanolkar, Joelle Hallak, Joy Sarkar, and Sandeep Jain

Purpose. We determined Semaphorin 7a (Sema7a) localization and abundance in naive corneas and in corneas after nerve-transecting lamellar flap surgery, and determined the effect of Sema7a supplementation on corneal nerve regeneration and inflammation.

Methods. Immunolocalization and Western blot analyses were performed to evaluate the abundance of Sema7a in naive corneas and corneas undergoing nerve regeneration after lamellar corneal surgery in *thy1*-YFP+ neurofluorescent mice. We used compartmental cultures of dissociated trigeminal ganglion cells to determine the effect of Sema7a exposure on neurite outgrowth in vitro. Finally, a Sema7a pellet was implanted under the corneal flap after lamellar transection surgery to determine the neuronal and inflammatory effects of Sema7a supplementation in vivo.

Results. Sema7a was expressed in the corneal epithelium and stromal keratocytes, but was more abundant in the epithelium (74.3%) compared to the stroma (25.7%, $P = 0.02$). Sema7a expression was increased significantly in the cornea after lamellar corneal surgery and was localized to stromal cells near the regenerating nerve fronds. Exposure of trigeminal neurites to Sema7a (20 nM) in the side compartment increased neurite length significantly. The implanted Sema7a pellet increased significantly YFP+ inflammatory cell influx into the cornea as well as increased corneal nerve length.

Conclusions. Sema7a is expressed constitutively in the cornea, and potently stimulates nerve regeneration and inflammatory cell influx. Therefore, this immune semaphorin links nerve regeneration and inflammatory processes in the cornea. (*Invest Ophthalmol Vis Sci.* 2012;53:4575–4585) DOI: 10.1167/iovs.12-9760

Inflammation has an essential role in peripheral nerve regeneration.[1] In the cornea, several recent reports have demonstrated interactions between injured nerves and the innate immune system. Li et al. reported a beneficial role for a γδ T cell-dependent inflammatory cascade involving IL-17, neutrophils, platelets, and VEGF-A in corneal nerve regeneration.[2] A strong, significant correlation has been reported between increased numbers of dendritic-shaped cells of the central cornea and decreased subbasal corneal nerves, suggesting a potential interaction between the immune and nervous systems in the cornea.[3] In addition, we reported previously that immunomodulation with cyclosporine eye drops reduces cytokine expression in the cornea and retards regenerative sprouting from transected corneal stromal nerve trunks.[4] Our data also revealed that topical benzalkonium application to the eye increased corneal inflammation and induced neurotoxocity.[5] Taken together, these results suggest that an optimal level of inflammation is required for corneal nerve regeneration, and excessive or insufficient inflammation has deleterious effects on this process. These findings suggest the presence of molecular regulators that straddle the immune and nervous systems in the cornea. These regulators, thus, affect nerve regeneration as well as the inflammatory response.

We reported recently the use of *thy1*-YFP transgenic mice for investigating corneal nerve regeneration after lamellar flap transection.[6] Using this mouse model, we evaluated the expression of nerve regeneration-associated genes and the neurotrophins.[7] We also examined the expression of the Eph/ephrin and Semaphorin family of nerve guidance proteins using qPCR array. We found that semaphorin 7a (Sema7a) was the only family member with increased expression at short- and long-term time points (unpublished data). Sema7a, also known as CD108, is a glycosylphosphatidylinositol (GPI)-anchored membrane-associated semaphorin.[8] In the nervous system, Sema7a promotes axonal outgrowth.[9] In the immune system, Sema7a expression is induced in activated T cells and is involved in T cell-mediated inflammatory immune responses.[10] In addition, we demonstrated previously that Sema7a recruits macrophages in vascularized corneas.[11] Sema7a functions in the nervous and immune systems via integrin-mediated signaling.[9,10] However, the role of Sema7a in corneal nerve regeneration has not been investigated to our knowledge. Therefore, we investigated whether Sema7a influences corneal nerve regeneration and recruits inflammatory cells to the cornea.

In our current study, we determined Sema7a localization and quantity in naive corneas, and during nerve regeneration after lamellar flap surgery. We also examined the effect of Sema7a supplementation on nerve regeneration and inflammation in vivo and in vitro. Our data suggested Sema7a is a physiologically relevant molecule that influences corneal nerve regeneration and inflammation processes.

Methods

Animals

All animal experiments were conducted in accordance with the ARVO Statement for the Use of Animals in Ophthalmic and Vision Research.

From the Corneal Neurobiology Laboratory, Department of Ophthalmology and Visual Sciences, University of Illinois at Chicago, College of Medicine, Chicago, Illinois.

Supported by National Eye Institute (NEI) Grant EY018874 (SJ), NEI core Grant EY001792, and Research to Prevent Blindness.

Submitted for publication February 27, 2012; revised May 16, 2012; accepted June 10, 2012.

Disclosure: **A. Namavari**, None; **S. Chaudhary**, None; **O. Ozturk**, None; **J.-H. Chang**, None; **L. Yco**, None; **S. Sonawane**, None; **N. Katam**, None; **V. Khanolkar**, None; **J. Hallak**, None; **J. Sarkar**, None; **S. Jain**, None

Corresponding author: Sandeep Jain, Department of Ophthalmology and Visual Sciences, University of Illinois at Chicago, 1855 W. Taylor Street, Chicago, IL 60612; jains@uic.edu.

The animal protocol was approved by the Institutional Animal Care and Use Committee (IACUC) of the University of Illinois at Chicago. *Thy1*-YFP (yellow fluorescent protein) neurofluorescent homozygous adult mice (6–8 weeks old) were purchased from Jackson Laboratories (Bar Harbor, ME), and colonies were established by inbreeding. For in vivo experiments, mice were anesthetized with intraperitoneal injections of ketamine (20 mg/kg; Phoenix Scientific, St. Joseph, MO) and xylazine (6 mg/kg; Phoenix Scientific). For terminal experiments, mice were sacrificed according to the IACUC protocol.

Animal Surgery

Surgery was performed on the left eye of each animal as described previously.[6] The central cornea was marked with a 2 mm-diameter disposable trephine (Visipunch; Huot Instruments, Menomonee Falls, WI). A partial-thickness incision (0.2 mm in length) was made perpendicular to the corneal surface and tangential to the circular trephine mark using a 15°, 5.0-mm standard angle knife (I-Knife model number 8065401501; Alcon, Fort Worth, TX). The peripheral lip of the corneal incision was depressed to penetrate the stroma centripetally, creating a corneal pocket. A 1.0-mm paracentesis knife (Clearcut Sideport model number 8065921540; Alcon) was used to expand the corneal pocket to the 2 mm-diameter trephine mark. Next, a 45°, 1.75-mm subretinal spatula (Grieshaber UltraSharp model number 682.11; Alcon) was used to enter the corneal pocket, incise it from within (ab-interno), and exit out at the 2 mm-diameter trephine mark. Vannas scissors then were used to extend the circumferential incision along the trephine mark. At three areas (each approximately 0.5 clock hours), the corneal pocket was left unincised. This formed three hinges that allowed the flap to remain attached to the cornea in the absence of sutures.

For in vivo Sema7a supplementation experiments, pellets containing recombinant mouse Sema7a-Fc were prepared and implanted in five eyes under the corneal flap adjacent to the superotemporal hinge. Five eyes received control Fc pellets. Pellets contained slow-release polymer Hydron (polyhydroxyethylmethacrylate), sucralfate (45 ng/pellet; Sigma-Aldrich, St. Louis, MO) and recombinant mouse Sema7a-Fc (100 ng/pellet; catalog number 1835-S3; R&D Systems, Minneapolis, MN) as described previously.[11,12] A suspension of recombinant Sema7a-Fc and sucralfate was prepared in sterile saline and concentrated for 10 minutes, and then 12% Hydron in 10 μL ethanol was added. The suspension then was deposited onto a sterilized nylon mesh and embedded between the fibers. The resulting grid (10 × 10-mm squares) was dried on a sterile Petri dish for 1 hour. The fibers of the mesh were separated under a microscope and from the approximately 100 pellets produced, 30–40 pellets of uniform size (0.4 × 0.4 × 0.2 mm) were selected for implantation. Animals received antibiotic ointment in the eye and underwent suture tarsorrhaphy, which was opened after 3 days. Bright field images were taken to ensure corneal clarity over the course of the study.

In Vivo Stereofluorescent Microscopy

Serial imaging was performed using a fluorescence stereomicroscope (StereoLumar V.12; Carl Zeiss Microscopy, Thornwood, NY) equipped with a digital camera (Axiocam MRm) and software (Axiovision 4.0) as described previously.[6] An anesthetized mouse was placed on the stereoscope stage. A total of 7 μL of proparacaine (0.5%; Bausch & Lomb, Tampa, FL) was applied for 3 minutes, and the pupil was constricted with 0.01% carbachol (Miostat; Alcon) for 5 minutes. Z-stack images were obtained at 5-μm intervals and compacted into one maximum intensity projection (MIP) image after alignment using Zeiss Axiovision software. A 1-mm diameter circular contour was drawn around the pellet and tangential to its peripheral edge. Within the contour, nerve fibers were traced manually using Neurolucida software (MBF Bioscience, Williston, VT). Neuroexplorer software (Nex Technologies, Littleton, MA) was used to measure the total nerve fiber length (NFL). The total number of YFP+ cells within the same contour was counted.

Corneal Whole-Mount Preparation and Confocal Microscopy

Mice were sacrificed one week after pellet insertion and corneal whole mounts were prepared. Corneas were excised and fixed directly in 4% paraformaldehyde (PFA) for 1 hour. After four 15-minute washes with PBS, corneas were mounted onto glass slides with a drop of 4′,6-diamidino-2-phenylindole (DAPI)-containing mounting medium and covered with a coverslip. All steps were performed at room temperature. To study the corneal nerve topography, we acquired confocal Z-stack images of corneal whole-mounts and performed 3D reconstruction using a LSM 510 META confocal microscope (Carl Zeiss Meditec, GmbH, Hamburg, Germany).

Corneal Immunostaining

Two weeks after surgery, three corneas were excised and processed for whole-mount immunofluorescence staining. Corneas were fixed in 4% PFA overnight at 4°C and washed four times with PBS (15 minutes each). Corneas then were permeabilized and blocked overnight at 4°C in 1% Triton X-100, 1% BSA, and 10% normal donkey serum in PBS. The corneas were incubated for 48 hours at 4°C with the primary antibody diluted in blocking solution (1:100), washed four times in PBS (15 minutes each), and incubated overnight at 4°C with the secondary antibody diluted in blocking solution (1:350). Corneas were washed, mounted on glass slides in mounting medium containing DAPI, and covered with a coverslip. The primary antibody was rabbit polyclonal anti-Semaphorin 7a (catalog number 23578; Abcam, Cambridge, MA). The secondary antibody was Dylight 594-conjugated AffiniPure donkey anti-rabbit IgG (Jackson ImmunoResearch, West Grove, PA).

Whole eyes were removed, and processed for sectioning and immunostaining. For Sema7a staining (3 eyes), eyes were embedded directly in optimal cutting temperature media (OCT; Tissue-Tek, Torrance, CA) and frozen on dry ice. For other stainings (4 eyes), whole eyes were first pre-fixed in 4% PFA overnight at 4°C, washed 3 times with PBS (15 minutes each), embedded in OCT, and frozen on dry ice. Specimens were cryosectioned into 8 μm-thick sagittal slices and mounted onto glass slides (R 7200; Mercedes Medical, Sarasota, FL). Sections were post-fixed in 4% PFA for 20 minutes at room temperature, washed 3 times with PBS (5 minutes each), and permeabilized and blocked for 1 hour at room temperature in 1% Triton X-100, 1% BSA, and 10% normal donkey serum in PBS. The sections were incubated overnight at 4°C with the primary antibody diluted in blocking solution (1:100), washed 3 times in PBS (5 minutes each), and incubated for 1 hour at room temperature with the secondary antibody diluted in blocking solution (1:350). After washing 3 times in PBS (5 minutes each), sections were coated with a drop of DAPI-containing mounting medium and covered with a coverslip. Primary antibodies were rabbit polyclonal anti-Semaphorin 7a, mouse anti-CD11b clone M1/70 (catalog number 13-0112-82; eBioscience, San Diego, CA), and purified Armenian hamster anti-mouse CD3ε clone 145-2C11 (catalog number 100302; BioLegend, San Diego, CA). The secondary antibodies were Dylight 594-conjugated AffiniPure donkey anti-rabbit, anti-mouse, and anti-Armenina hamster IgG, respectively (Jackson ImmunoResearch). Dylight 594 was chosen to ensure no overlap with the YFP wavelength and to minimize false-positive staining. Isotype control and omission of primary antibody were used to ensure staining specificity. Z-stack or single-plane images of corneal whole-mounts or sections were obtained using a LSM 510 META confocal microscope.

Real-Time Quantitative PCR

Two weeks after surgery, corneas were harvested, and Sema7a and growth-associated protein 43 (Gap43) were analyzed by real-time

quantitative PCR (qPCR). Six pairs of corneas from six mice were processed separately for RNA extraction and qPCR; the right cornea of each mouse was used as the control for the left cornea (which received the surgery) to minimize the potentially confounding effect of innate variability in gene expression. All primers and reagents were purchased from SABiosciences (Frederick, MD) unless specified otherwise. The primers used were Sema7a (catalog number PPM41378A), Gap43 (catalog number PPM03303A), and glyceraldehyde-3-phosphate dehydrogenase (GAPDH, catalog number PPM02946E). The central cornea was marked with a trephine, incised with scissors, and placed directly in Trizol (Invitrogen, Carlsbad, CA) for RNA extraction, which was conducted according to the manufacturer's protocol. Reverse transcription was performed with 50 ng total RNA using the RT^2 First Strand cDNA Synthesis kit. The resulting cDNA was preamplified using the RT^2 Nano PreAMP Kit according to the manufacturer's instructions. Real-time qPCR was performed with SYBR using a 7900HT ABI real-time instrument (Applied Biosystems, Foster, CA). Samples were assayed in triplicate in a total volume of 25 μL using thermal cycling conditions of 10 minutes at 95°C, followed by 40 cycles of 95°C for 15 seconds, and 60°C for 60 seconds. A mouse genomic DNA contamination control was used to confirm that DNA contamination did not occur in amplification reagents. For data analyses, the cycle threshold (CT) of each gene for the surgery eye was normalized to the corresponding value for the control eye and used to calculate the fold change with the $2^{-\Delta\Delta CT}$ method.

Isolation and Culture of Corneal Cells

Corneas of *thy1*-YFP mice were excised and the stromal cells were isolated using a modification of three sequential collagenase digestions as described previously.[13] The isolated stromal cells were cultured in keratocyte, fibroblast, or myofibroblast induction media. Keratocytes were cultured in serum-free Dulbecco's modified Eagle's medium (DMEM)/F12. Fibroblasts were cultured in media containing 10 ng/mL recombinant basic FGF (R&D Systems). Myofibroblasts were cultured in media containing 10 ng/mL recombinant TGF-β 1 (R&D Systems). Confluent stromal cells were lysed in modified RIPA cell lysis buffer (20 mM Tris·HCl, pH 7.4; 150 mM NaCl; 1 mM EDTA; 1 mM EGTA; 1% IGEPAL; 2.5 mM sodium pyrophosphate; 1 mM β-glycerophosphate, pH 7.4) and processed for immunoblot analyses.

Immunoblot Analyses

Pooled excised normal or 2-week post-surgery corneas (7 corneas/group) were snap-frozen in liquid nitrogen and homogenized in modified RIPA cell lysis buffer supplemented with a complete protease inhibitor, and a phosphatase inhibitor cocktail I and II (Sigma Chemical Co., St. Louis, MO) using a Biopulverizer (Biospec Products Inc., Bartlesville, OK). Cultured cells were transferred directly to the same cell lysis buffer. Samples were centrifuged at 10,000 times gravity for 15 minutes at 4°C and the supernatant was collected. Total protein was determined using a modified Lowry method (BioRad DC Protein assay; BioRad Laboratories, Hercules, CA). For Western blot analyses, 100 μg total protein or recombinant mouse Sema7a-Fc (10, 25, and 50 ng; catalog number 1835-S3; R&D Systems) were separated electrophoretically on 4–12% Tris–Glycine SDS polyacrylamide gels (XCell SureLock Mini-Cell Electrophoresis System; Invitrogen). Samples were transferred to 0.2-μm nitrocellulose membranes (Whatman Inc., Florham Park, NJ) by electro-elution. Membranes were blocked in Li-Cor blocking buffer (Li-Cor Biosciences, Lincoln, NE), followed by an overnight incubation at 4°C with rabbit polyclonal anti-Sema 7a (diluted 1:500 in blocking buffer). Mouse monoclonal anti-GAPDH (diluted 1:2000; Santa Cruz Biotechnology, Santa Cruz, CA) was used as a loading control. After three 10-minute washes in PBS containing 0.1% Tween-20, the blots were incubated for 2 hours at room temperature in the fluorescently-labeled secondary antibody mixture of goat anti-rabbit (IRDye800CW, 1:15,000 dilution in blocking buffer) and goat anti-mouse (IRDye700DX, 1:10,000 dilution in blocking buffer) antibodies (Rockland Immunoresearch, Gilbertsville, PA). Membranes were imaged using LiCor Odyssey Infrared imager (Li-Cor Biosciences). The relative intensity of each band (normalized to GAPDH) was determined using the LiCor Odyssey application software for quantification. Data are expressed in arbitrary units as the relative abundance of Sema7a.

Compartmental Culture of Dissociated Trigeminal Ganglion Cells

Trigeminal ganglion neurons were isolated from 10-day-old *thy1*-YFP pups and compartmental cultures were performed as described previously.[4,5] The central compartment was filled with F12 media containing 10% fetal calf serum (FCS), 1% penicillin-streptomycin, nerve growth factor (NGF) (2.3 μM), and AraC (0.3 μM). Side compartments were filled with the same media lacking AraC and NGF. Recombinant mouse Sema7a-Fc (20 nM, catalog number 1835-S3; R&D Systems) or vehicle (PBS) was added to side compartments on day 3. The Sema7a-Fc concentration was selected based on studies by Pasterkamp et al.[9] On day 5, images of neurite outgrowth along the tracks were acquired. All images were analyzed using Neurolucida software.

Neurite Outgrowth Analyses

After 3 days in culture, neurites extended from cell bodies in the central compartment and crossed the Teflon divider to reach the side compartment tracks. NFL was measured in each track using Autoneuron software (MBF Bioscience). NFL was calculated on day 5 after vehicle or Sema7a-Fc treatment. In vitro experiments were terminated on day 5.

In Vitro Potency of Sema7a and NGF

Dissociated trigeminal neuronal cells were plated on collagen coated plates. Cells were treated with 2, 20, and 200 nM, and 2 μM of either NGF or Sema7a-Fc. Control plates were treated with vehicle. After 48 hours, the NFL/soma was calculated for each group (Control, Sema7a-Fc, and NGF) using Autoneuron software.

Statistical Analyses

Statistical analyses were performed using Microsoft Excel (Microsoft, Redmond, WA). Student's *t*-test was used to compare mean values between groups. Results are shown as mean ± SEM. Differences were considered significant if $P < 0.05$.

Results

Sema7a Expression, Abundance, and Localization in the Naive Cornea

Previous studies have suggested the presence of molecular regulators that function in the nervous and immune systems. We hypothesized that Sema7a, an immune semaphorin, might be one of these regulators. Therefore, we evaluated the expression and localization of Sema7a in the cornea. Sema7a was localized in the corneal epithelium and stromal keratocytes as determined by immunostaining (Fig. 1A1). The endothelium showed very weak immunostaining. The antibody was specific for Sema7a as shown by absence of immunostaining in the isotype control image (Fig. 1A2). Quantitative Western blot analyses were performed using increasing quantities of recombinant Sema7a-Fc to determine the band intensity produced by a given amount of Sema7a-Fc (Fig. 1B). The rabbit polyclonal Sema7a antibody detects a 75-kDA protein band. We observed additional bands at ~50 and 100

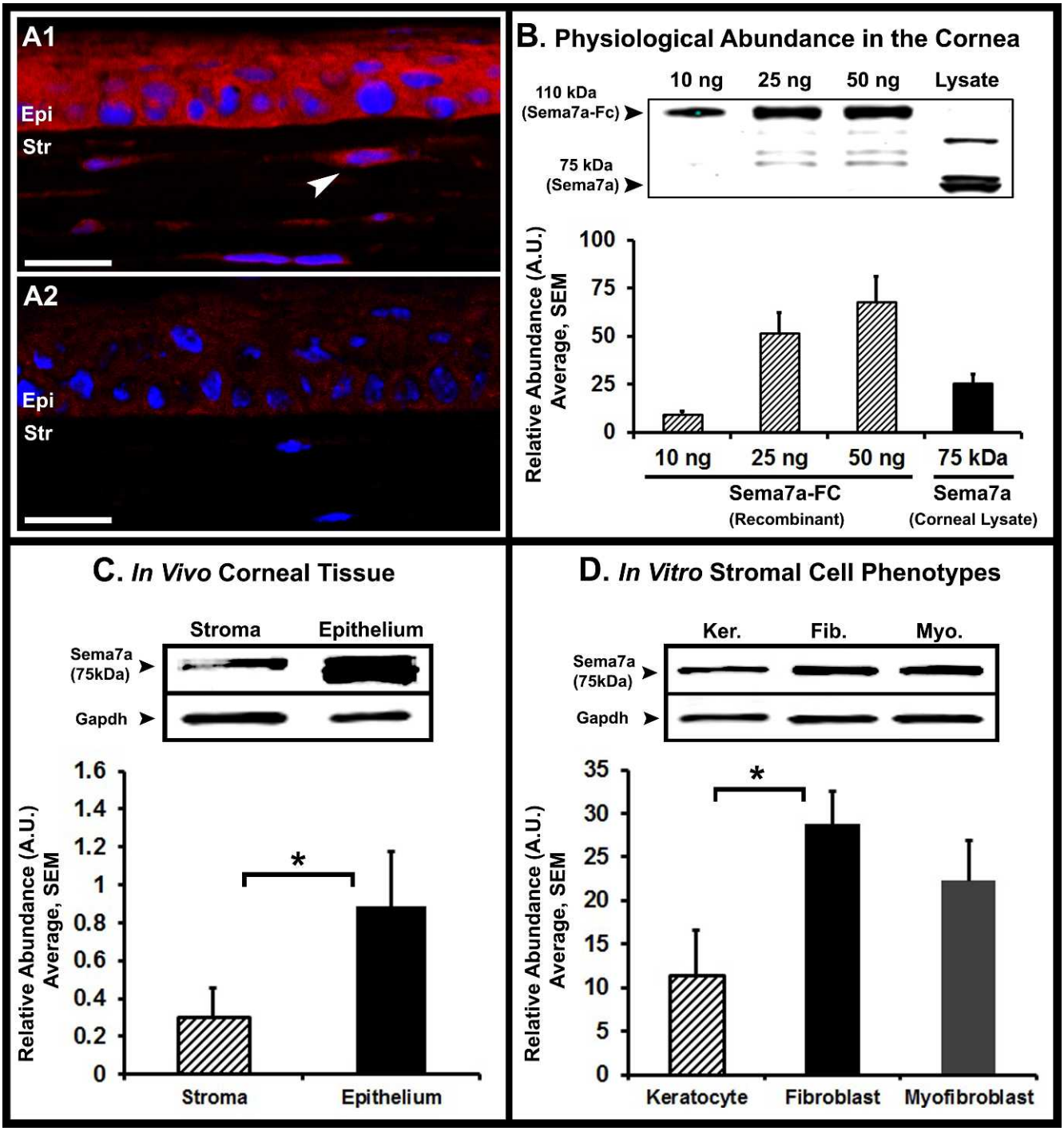

Figure 1. Localization and abundance of Sema7a in naive corneas. (**A1**) Confocal immunofluorescence image showing Sema7a (*red*) localizes to the epithelium (*epi*) and stroma (*str*). *Arrowhead*: indicates a Sema7a+ stromal keratocyte. (**A2**) The absence of immunostaining in isotype control is shown (image was taken at identical confocal settings). White scale bar, 20 μm. (**B**) The physiological abundance of Sema7a in naive corneas as determined by quantitative Western blot analyses. Although the Sema7a antibody detects nonspecific bands, the Sema7a protein is detected at 75 kDa. Sema7a-Fc is detected at 110 kDa. Based on the band intensity of Sema7a from lysates of pooled corneas, we determined that of the abundance of Sema7a is 56.6 ng/per naive cornea. (**C**) Quantitative Western blot analyses of naive corneas indicates that Sema7a is more abundant in the epithelium than stroma. (**D**) Quantitative Western blot analyses of cultured corneal stromal cells demonstrates that fibroblasts and myofibroblasts are more abundant in Sema7a than keratocytes. Western blot images presented are representative of three separate experiments. Error bars represent SEM. $^*P < 0.05$.

kDa, which are likely to be cleavage fragments and a glycosylated form, respectively. In this study, we analyzed only the 75-kDa band. One nanogram of Sema7a-Fc (~100 nM) produced a band intensity of 1.094 arbitrary units (AU). To determine the physiological quantity of Sema7a in a lysate of pooled corneas, the band intensity (AU) was measured and the abundance was calculated using the conversion of 1.094 AU = 1 ng. The amount of Sema7a in naive corneas was determined

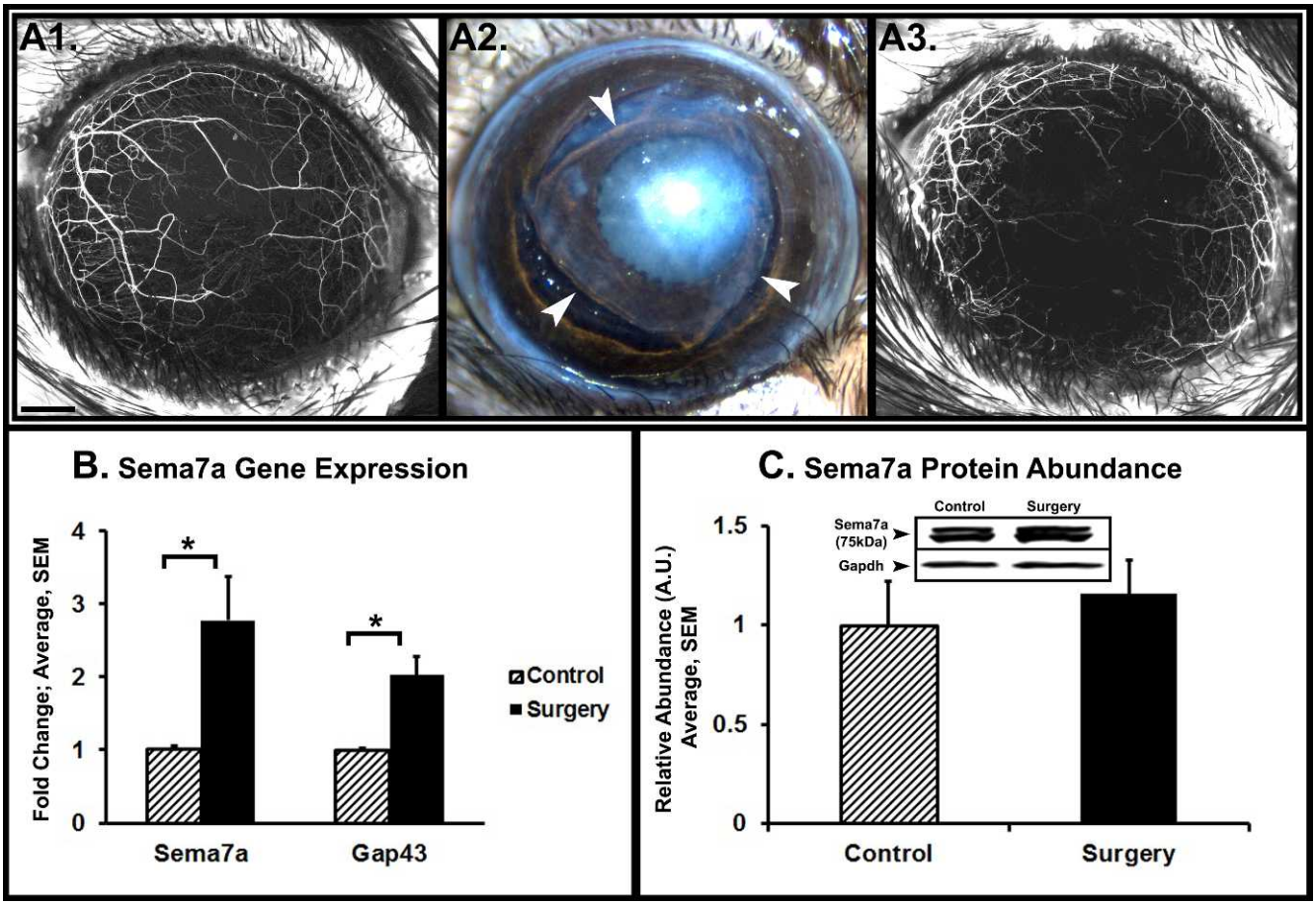

Figure 2. Sema7a expression and abundance after nerve transecting lamellar corneal surgery. (**A1**) Stereofluorescent microscope image of a naive cornea with fluorescent nerves. Black scale bar, 500 μm. (**A2**) Image of cornea immediately after lamellar flap surgery. *Arrowheads*: indicate the edges of the flap. (**A3**) The same cornea 2 weeks after surgery shows early evidence of nerve regeneration. (**B**) Real-time quantitative PCR on corneas 2 weeks after lamellar flap surgery. The graph depicts significantly increased Sema7a and Gap43 gene expression. (**C**) Western blot analyses of corneas 2 weeks after lamellar flap surgery show that Sema7a abundance increased by 16%. The data presented are representative of three separate experiments. A representative Western blot image is shown. Error bars represent SEM. $^*P < 0.05$.

to be 56.6 ng/cornea. We determined the concentration of Sema7a using the molecular weight of Sema7a and the corneal volume. The mouse cornea has an average diameter of 2.6 mm and thickness of 100 μm, one-third of which is epithelium and two-thirds is stroma.[14,15] The mouse cornea is circular, not oval-shaped like the human cornea.[15] Therefore, we determined the corneal volume using the formula for a cylinder, $\pi r^2 h$. The concentration of epithelial Sema7a was 2.38 μM, and in the stroma it was 0.41 μM.

Next, using whole corneas, we determined the relative proportion of Sema7a in the epithelium and stroma (Fig. 1C). We compared the band fluorescence intensity of Sema7a in the epithelium (0.88 ± 0.3) and stroma (0.30 ± 0.1) relative to GAPDH. We determined that Sema7a was significantly more abundant in the epithelium (74.3%) than the stroma (25.7%, $P = 0.02$).

Finally, we evaluated whether Sema7a abundance differs in naive resident stromal cells (keratocytes) versus wound healing phenotypes (fibroblasts and myofibroblasts) (Fig. 1D). We used media containing bFGF to induce a fibroblast transformation and TGF-β1 to induce a myofibroblast transformation in cultured keratocytes. Sema7a was significantly more abundant in the fibroblasts (28.79 ± 3.7) compared to keratocytes (11.49 ± 5.1, $P = 0.03$). Sema7a abundance in myofibroblasts (22.30 ± 4.63) also was greater than in keratocytes; however, the difference was not significant ($P = 0.09$).

Sema7a Expression, Abundance, and Localization during Cornea Nerve Regeneration

To determine Sema7a expression and abundance during cornea nerve regeneration, lamellar corneal surgery was performed to transect corneal nerves. We used stereofluorescent microscopy to visualize the corneal nerves. YFP fluorescence disappears in transected stromal nerves distal to the transection site (Figs. 2A1, 2A2). Subsequent nerve regeneration was visualized by reappearance of YFP fluorescence. Two weeks after surgery, corneas showed evidence of regeneration (Fig. 2A3). We performed quantitative PCR on whole corneas to determine Sema7a gene expression (Fig. 2B). Compared to unoperated control corneas (1.03 ± 0.03), Sema7a expression was significantly increased in operated corneas (2.78 ± 0.6, $P = 0.05$). The expression of Gap43, a nerve regeneration-associated gene, also was increased significantly in operated corneas, confirming nerve regeneration activity. Western blot analyses showed that Sema7a protein abundance increased by 15.8% in operated corneas compared to control corneas (Fig. 2C).

Whole mount immunofluorescent staining of corneas was performed to determine Sema7a localization in regenerating corneas (Fig. 3A). We observed Sema7a staining in the vicinity of regenerating nerve fronds (Fig. 3B) and Sema7a was localized to stromal cells (Fig. 3B2, arrowhead). In unoperated

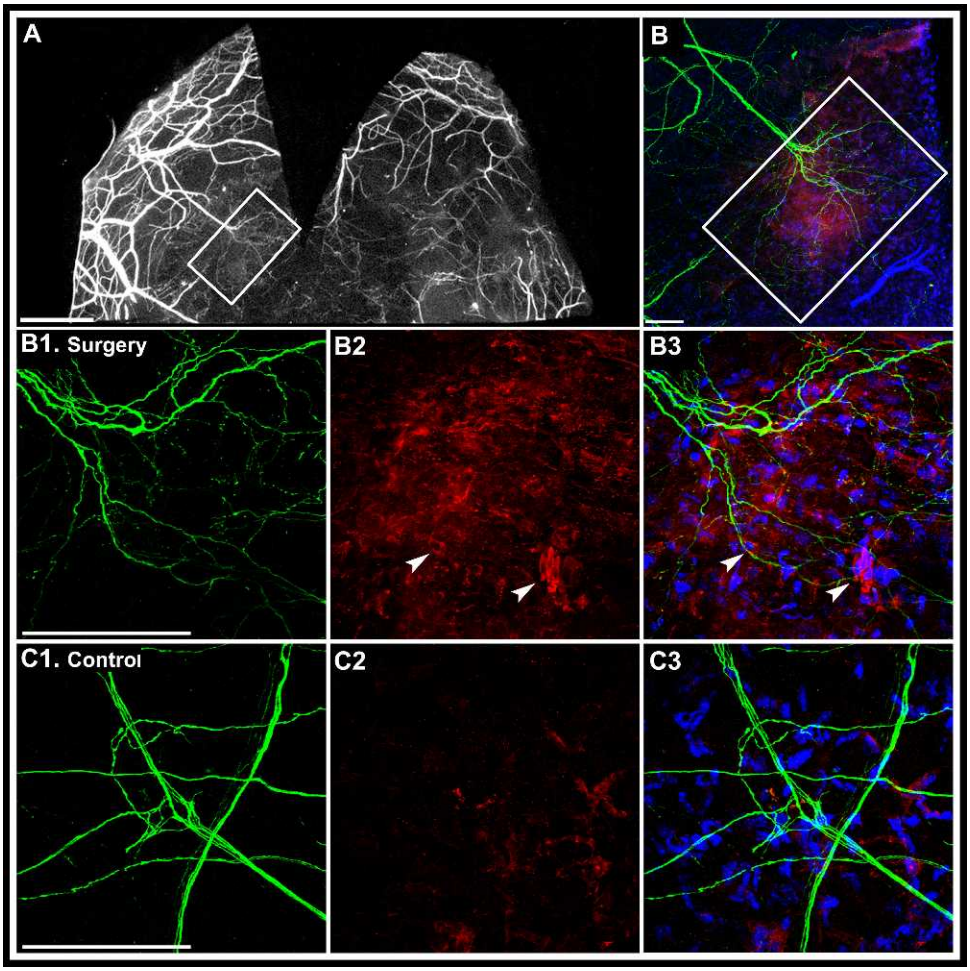

Figure 3. Sema7a localization in corneal whole mounts 2 weeks after lamellar flap surgery. The flap was removed to allow better antibody access to stroma. The stromal area boxed in panels (**A**) and (**B**) is shown at higher magnification in panels (**B1**), (**B2**), and (**B3**). (**A**) Wide-field fluorescent microscope image shows regenerating nerve fronds emanating from a transected stromal nerve (*boxed white rectangle*). White scale bar, 1000 μm. (**B**) Confocal immunostaining of the same boxed area shows regenerating nerve fronds (*green*) and Sema7a staining (*red*) at lower magnification. (**B1–B3**) Confocal immunostaining image of the center of boxed area at higher magnification. (**B1**) Regenerating nerve fronds. (**B2**) Sema7a staining (*red*). *Arrowheads*: indicate stromal cells with membrane Sema7a localization). (**B3**) An overlay with DAPI to indicate nuclear staining. (**C1–C3**) Control corneas. (**C1**) A normal pattern of stromal nerves. (**C2**) Sparse Sema7a staining in the stroma. (**C3**) An overlay with DAPI nuclear staining. White scale bars for panels (**B**), (**B1**), and (**C1**), 100 μm.

control corneas (Figs. 3C1–3C3), Sema7a was expressed weakly and localized sparsely to stromal cells.

Neuronal Effect of Sema7a on Neurite Outgrowth In Vitro and Potency Comparison with NGF

To determine the effect of Sema7a exposure on neurons, we used compartmental cultures of dissociated trigeminal ganglion cells (Fig. 4). Exposure of 20 nM Sema7a to trigeminal neurites in the side compartment significantly increased neurite length (70.06 ± 6.0 mm, $P < 0.001$) compared to vehicle control (23.06 ± 1.18 mm, Figs. 4A1–4A3). Next we evaluated the potency of Sema7a on neurite growth on cultured trigeminal ganglion cells, and compared it to equimolar NGF, the prototypical neurotrophic factor (Figs. 4B1, 4B2). At the 20 nM concentration, Sema7a (2.23 ± 0.26 mm/cell) and NGF (2.27 ± 0.35 mm/cell) exhibited maximal neurite growth that was significantly greater than vehicle control (1.0 ± 0.09, $P < 0.05$). In addition, the potency of Sema7a and NGF was similar at this concentration (~1% difference). However, at lower (2 nM) or higher (200 nM and 2 μM) concentrations, the potency of NGF consistently was higher than Sema7a (range 15.2–26%) but the differences were not statistically significant.

In Vivo Neuronal and Inflammatory Effects of Sema7a

To determine the effects of Sema7a supplementation on neurons and inflammation in vivo, we performed lamellar transection surgery (Figs. 5A1, 5A2) and implanted a Sema7a pellet (100 ng/pellet; Figs. 5B1, 5B2) or vehicle pellet (Figs. 5C1, 5C2) under the corneal flap. The Sema7a pellet significantly increased the influx of YFP+ inflammatory cells as well as significantly increased corneal nerve length. The observed number of YFP+ inflammatory cells in the Sema7a pellet group (89.6 ± 23.8) was significantly greater than the vehicle pellet group (36.2 ± 14.3, $P = 0.04$). The regenerated corneal nerve length in the Sema7a pellet group (89.6 ± 23.8) also was significantly greater than the vehicle pellet group (36.2 ± 14.3, $P = 0.01$). The YFP+ inflammatory cells were CD45-positive, thus confirming their hematopoietic lineage. The inflammatory cells also were CD11b- and CD3-positive (Figs. 5G, 5H). We obtained 3D reconstructed Z-stack images of

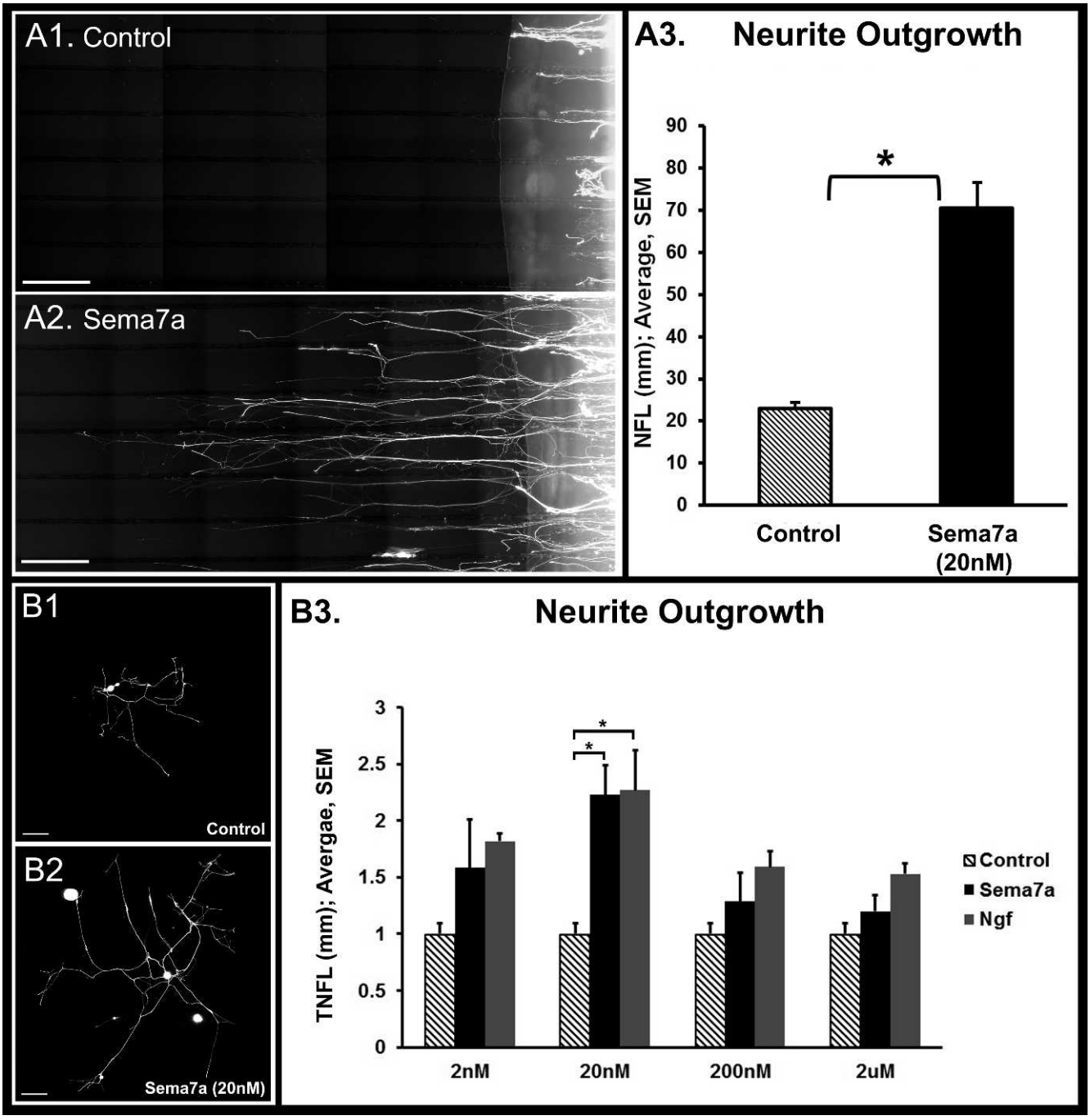

Figure 4. Effect of Sema7a on neurite outgrowth in vitro. (**A1**, **A2**) Compartmental cultures of dissociated trigeminal ganglion cells were performed. The image shows the side compartment with neurites growing over collagen-etched parallel tracks. Neurite growth was significantly greater with Sema7a-Fc supplementation in the side compartment compare to vehicle supplementation (**A3**). White scale bar for (**A1**) and (**A2**), 500 μm. (**B1–B3**) The potency of Sema7a on neurite growth was compared to NGF. Trigeminal ganglion cells with Sema7a supplementation (**B2**) showed significantly greater neurite growth compared to vehicle (**B1**). Total nerve fiber length (*TNFL*) at different equimolar concentrations of Sema7a-Fc or NGF. Maximal neurite growth was observed at 20 nM for Sema7a-Fc and NGF. The potency of Sema7a and NGF was similar at 20 nM. Error bars represent SEM. $^*P < 0.05$. White scale bar for (**B1**) and (**B2**), 200 μm.

corneal whole mounts using confocal microscopy to determine the anteroposterior arrangement of nerves (Figs. 5D1–5D3). In naive corneas, the nerves were arranged in two layers, an anterior subbasal and a posterior stromal layer (Fig. 5D1). After Sema7a pellet implantation, long regenerating nerves were seen in the subbasal area (Fig. 5D2). After vehicle pellet implantation, regenerating nerves were observed in the mid-stroma near the flap interface, similar to our previous report (Fig. 5D3).[6]

Discussion

Our study yielded four important findings. First, we determined that Sema7a is expressed constitutively in the cornea, mainly

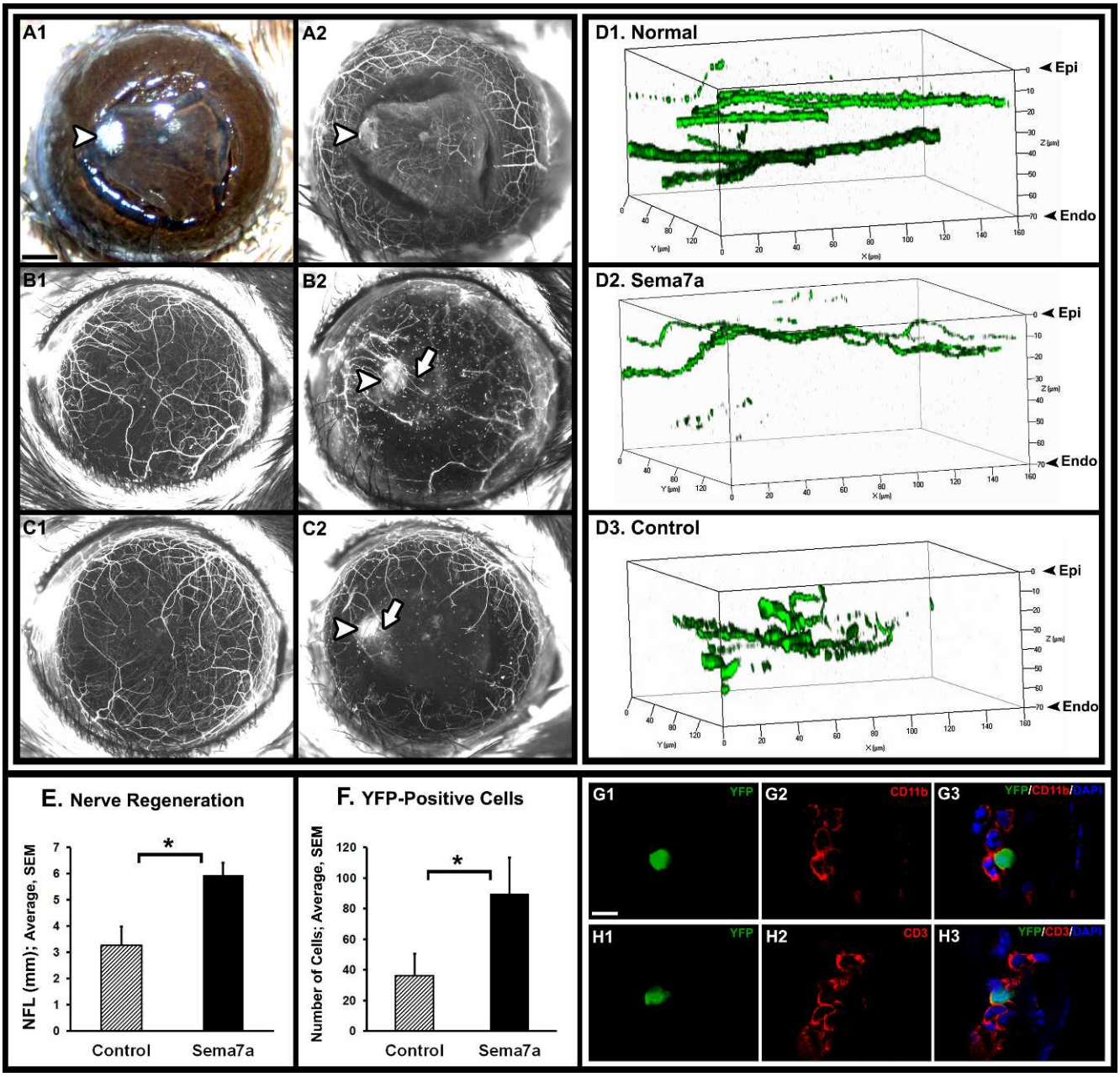

Figure 5. Effect of Sema7a on nerve regeneration in vivo. Lamellar flap surgery was performed and a pellet containing either Sema7a-Fc (**B**) or vehicle (**C**) was implanted under the flap, adjacent to the flap hinge. (**A1**) Color photograph of a corneal flap immediately after surgery. *Arrowhead*: indicates implanted pellet. (**A2**) Stereofluorescent microscope image of the same cornea. (**B1**, **B2**) Stereofluorescent image of a cornea pre-surgery (**B1**) and 1 week after implantation with Sema7a pellet (**B2**). *Arrowhead*: indicates the implanted pellet. *Arrow*: shows regenerating nerves. Nerve regeneration is robust and extends beyond the pellet. (**C1**, **C2**) Stereofluorescent image of a cornea pre-surgery (**C1**) and 1 week after implantation with vehicle pellet (**C2**). *Arrowhead*: indicates the implanted pellet. *Arrow*: shows regenerating nerves. There is less nerve regeneration and it is adjacent to pellet. (**D1–D3**) Confocal microscopy was used to obtain 3D reconstruction of Z-stack images. (**D1**) In naive cornea the nerves are arranged in 2 layers, a subbasal layer under the epithelium (*Epi*) and a deeper stromal layer. (**D2**) After Sema7a pellet implantation, long regenerating nerves were observed in the subbasal area. (**D3**) After vehicle pellet implantation, regenerating nerves were deeper in the stroma (near the flap interface). (**E**) NFL was significantly greater with the implanted Sema7a pellet compared to the implanted control pellet. (**F**) The number of YFP+ cells in the cornea was significantly greater in Sema7a pellet corneas compared to control pellet corneas. (**G1–G3**) Confocal images of corneal immunostaining with the CD11b antibody shows that CD11b (*red*) co-localizes with YFP+ cells (*green*). (**H1–H3**) Confocal images of corneal immunostaining with the CD3 antibody shows that CD3 (*red*) co-localizes with YFP+ cells (*green*). Error bars represent SEM. $^*P < 0.05$, White scale bar for (**G**) and (**H**), 10 μm.

concentrated in the epithelium with less expression in the stroma. Second, we found that corneal Sema7a expression increases after nerve transecting lamellar surgery and is localized near the regenerating nerve fronds. We also determined that Sema7a induces neurite growth in vitro as potently as NGF. Finally, Sema7a induced significant nerve regeneration in vivo that was accompanied by significant inflammatory cell influx to the cornea. Taken together, these findings suggest Sema7a acts as a neurotrophic factor in the cornea that also can influence inflammatory processes. Integrin-mediated signaling

is a common mechanism by which Sema7a links the nervous and immune systems.[9,10] In the nervous system, Sema7a promotes axon outgrowth through β1 integrin receptors.[9] In the immune system, Sema7a stimulates macrophage production of proinflammatory cytokines through α1β1 integrin.[10]

Semaphorins were identified originally as axon guidance factors. However, unlike many semaphorins that act as repulsive guidance cues, the GPI-anchored membrane-associated Sema7a is neither an axonal repellent nor attractant.[9] Instead, it promotes axon outgrowth in a direction that likely is dictated by other cues. It now is known that several semaphorins, the so-called "immune semaphorins," are involved in various phases of the immune response by regulating immune cell contacts or cell migration.[16,17] These "immune semaphorins" include Sema3A, 4A, 4D, 6D, and 7A.[16,17] In the immune system, Sema7a expression is induced on activated T cells. Sema7a stimulates monocytes and macrophages through α1β1 integrin, and increases production of proinflammatory cytokines, including IL-6 and tumor necrosis factor-α.[10] Recombinant soluble Sema7a is an extremely potent monocyte chemoattractant and also can induce monocytes toward a dendritic cell morphology.[18] Our current results are similar. Sema7a supplementation increased axonal length significantly and increased the influx of inflammatory cells. These inflammatory cells included CD11b-positive monocytes and macrophages, as well as CD3-positive lymphoid lineage cells. Although we were investigating molecular regulators of corneal nerve regeneration, we also discovered that in *thy1*-YFP transgenic neurofluorescent mice, some bone marrow-derived hematopoietic lineage cells also are fluorescent. The discovery of fluorescent non-neuronal inflammatory cells was unexpected because the *thy1*-YFP mouse was generated using the neuronal thy1 gene promoter, not the non-neuronal elements.[19] Feng et al. also had observed a small number of occasional YFP-positive mononucleated cells in their transgenic lines, but did not characterize them.[19] The presence of YFP+ inflammatory cells in the *thy1*-YFP transgenic mouse provides a powerful tool for in situ visualization of nervous and inflammatory system interactions.

In the *thy1*-YFP mouse model, a proportion of sensory nerves are fluorescent, so axonal regeneration and degeneration can be visualized and quantified in vivo. Therefore, this eliminates the need for animal sacrifice and tissue processing for histochemical analyses.[20] This rationale forms the basis for several reports using the *thy1*-YFP model to investigate neuronal regeneration. For example, this animal model has been used to study regeneration after saphenous[21] or sciatic nerve[22] crush injury, traumatic axonal injury in the brain,[23] as well as degeneration after optic nerve crush injury.[24] The use of these mice for studying corneal nerves was reported first by Yu et al.[25] These investigators reported that only half of the corneal subbasal nerves are YFP labeled. We reported that changes in the density and pattern of the YFP-labeled subbasal nerve plexus may occur with sequential stereofluorescence microscope imaging without any intervention.[6] Therefore, investigation of the subbasal nerve plexus should account for any limitations inherent in the *thy1*-YFP mouse model as well in vivo visualization methodology limitations.

In contrast to the subbasal nerve plexus, nearly all stromal nerves can be visualized in the *thy1*-YFP mouse model.[25] The stromal nerves have YFP-labeled and unlabeled fibers; however, there are enough YFP-labeled fibers in each stromal nerve to allow their visualization. The pattern and density of stromal nerves remains constant during sequential visualization.[5,6] YFP fluorescence disappears in transected stromal nerves distal to the transection site and reappears in regenerating neurites.[25] By visualizing the density and pattern of regenerating YFP-labeled neurites, it is possible to investigate the neurotrophic potential of molecular or pharmacologic interventions on stromal nerve regeneration.[4] Given that all sensory fiber types (myelinated non-nociceptive and unmyelinated nociceptive) are present in the regenerating neurites,[6] regenerative sprouting from the transected stromal nerves provides a reliable estimate of nerve regeneration. In our current data, we performed lamellar dissection to transect stromal nerves. Subsequent nerve regeneration was visualized by the reappearance of YFP fluorescence and confirmed by a significant increase in expression of the prototype regeneration-associated gene, Gap43.

The Sema7a pellets used in our study were prepared using Hydron and sucralfate. Using similarly prepared pellets,[26] Tong et al. performed in vitro experiments to investigate release kinetics of rhodamine-labeled lactalbumin.[27] The release rate for a 50 ng pellet from day 8 to day 14 was 0.32% per day. Their data indicate that the release rate was insensitive to the dose of drug in the pellet but was significantly higher if sucralfate was absent, which was consistent with the properties of sucralfate reported in the literature.[27] These investigators used these data to determine the in vivo release kinetics of bFGF pellet implanted in the rat cornea.[27] Using this approach, we estimate that the release rate of Sema7a (100 ng/pellet) is 0.3 ng per day, equivalent to molarity of 14.7 nM in the cornea. The amount of Sema7a released from the pellets within the cornea approximates the in vitro concentration that produces maximal neurite outgrowth. After Sema7a pellet implantation, we observed long regenerating nerves in the subbasal location, whereas after vehicle pellet implantation, regenerating nerves were observed in the mid-stroma near the flap interface, similar to our previous report.[6] One explanation for this difference may be related to collagen IV, a major constituent of epithelial basement membranes, and its receptor, α1β1 integrin. Integrin α1β1 is expressed on macrophages and anchors them to extracellular matrix substrates. Adhesive interactions are crucial for cell migration and retention to inflammatory sites.[28] Sema7a exuding from the pellet may have bound α1β1 integrin receptors on collagen IV anchored macrophages in the epithelial basement membrane, thus stimulating nerve regeneration subbasal.

Our in vitro data showed greater Sema7a abundance in wound healing stromal cells (fibroblasts and myofibroblasts) than in naive resident stromal cells (keratocytes). The wound healing phenotypic cells were generated by exposing keratocytes to FGF (fibroblasts) or TGF-β1 (myofibroblasts). Our findings agree with the data reported by Kamata et al., which indicate that exposure of normal epidermal keratinocytes to TGF-β1 increased Sema7a gene expression.[29] In skin, it has been proposed that Sema7a expression on basal keratinocytes may interact directly and indirectly with immune cells infiltrating into the upper dermis as well as the epidermis. Our data indicated Sema7a is localized in epithelial cell membranes and the basement membrane. Therefore, we propose that, similar to the skin, Sema7a expression on basal epithelial cells potentially interacts with immune cells as well as regenerating nerves. Upon lamellar flap surgery, Sema7a localized to the stromal cells, which appeared fibroblast-like with confocal microscopy. It is likely that Sema7a on the fibroblast membrane interacts with immune cells and regenerating nerves in the flap interface.

Corneal nerve dysfunction is the pathophysiologic basis of ocular diseases that cause considerable morbidity, including neurotrophic keratitis and dry eye disease.[30,31] Several ophthalmic surgical procedures, such as corneal transplantation, photorefractive keratectomy (PRK), and laser-assisted in situ keratomileusis (LASIK), cause corneal nerve disruption, which can lead to neurotrophic epitheliopathy.[32] Despite the clinical need to promote corneal nerve regeneration in neurotrophic corneas, there are relatively few specific

therapeutic interventions.[33] Several neurotrophin and nerve regeneration-associated genes are expressed in the cornea. These include NGF, brain-derived neurotrophic factor (BDNF), neurotrophin 3 (NT3), and glial cell-derived neurotrophic factor (GDNF).[34,35] NGF is the prototypic neurotrophic factor that has been investigated in wound healing and promotes corneal epithelial healing. NGF also improves corneal allograft survival as well as causes faster corneal nerve regeneration.[36] In these studies, recombinant mature NGF (~13 kDa) was applied as eye drops. We were unable to detect mature NGF protein in unoperated or operated corneas by Western blot analyses (data not shown). Our finding is consistent with other reports showing that levels of mature NGF in peripheral tissues are negligible or undetectable.[37] In contrast to NGF, we were able to detect Sema7a in the normal cornea. Our data showed a significant increase in Sema7a gene expression, but not in protein abundance, after nerve transecting lamellar corneal surgery. This finding suggested that the level of Sema7a protein is regulated post-translationally. Our data are in agreement with that of a previous report showing that the Sema7a RNA and protein expression profiles are discordant, which is not the case for other semaphorins (including Sema3a or Sema3e).[38] Cell membrane anchored Sema7a is cleaved to a soluble form.[39] Sema7a protein is a substrate for matrix metalloproteinase-2 and Caspase-9,[40,41] proteases that are expressed in the cornea during wound healing or in response to stress.[42,43] These data indicate that Sema7a is likely regulated at the post-translational level by proteolytic cleavage and processing in the extracellular matrix.

Proteolytic cleavage of cell surface bound semaphorins has emerged as a potential mechanism for their biologic action. To exert its pro-angiogenic functions, Sema4D, a membrane-bound semaphorin, is cleaved by membrane type 1-matrix metalloproteinases and released into the surrounding environment as a soluble form to act in a paracrine manner on endothelial cells.[38] Semaphorin 3C, a secreted semaphorin, is cleaved by metalloproteinases to generate a soluble form that diffuses into the extracellular matrix to promote cell migration.[44] Cell membrane GPI-anchored Sema7a also is cleaved to form a soluble form in cell culture supernatants.[39] We were unable to differentiate between bound and soluble Sema7a in Western analysis of corneal lysates. The proteases cleave Sema7a very close to the GPI anchor and, therefore, the molecular weight of soluble Sema7a is similar to that of the membrane-bound protein.[39] The amount of Sema7a in the mouse cornea is 56.6 ng, of which 75% is in the epithelium and 25% is in the stroma. The concentration of Sema7a is 2.38 μM in epithelium and 0.41 μM in stroma. We calculated the concentration of Sema7a separately for the epithelium and stroma due to the large differences in their volumes and the amount of resident Sema7a. In addition, we determined that 20 nM Sema7a induces significant neurite growth in dissociated trigeminal ganglion cells in vitro, confirming previous reports of robust neurite growth with this concentration.[9] Higher concentrations of Sema7a resulted in lower neurite growth, in agreement with previous data.[45]

The 20 nM Sema7a concentration that potently stimulates nerve regeneration in vitro is approximately 20 times lower than the physiologic concentration found in the stroma and 120 times lower than that in the epithelium. One explanation for the apparent disparity in the physiologic amount of Sema7a in naive corneas and the biologically effective in vitro concentration is that in naive tissues, Sema7a is expressed as a membrane-bound protein, but in our in vitro experiments soluble Sema7a was used. The bioavailability of cell surface bound Sema7a for neuronal actions in corneal extracellular matrix may be limited. Our study demonstrates that Sema7a is expressed constitutively in the corneal epithelium and stroma in sufficient quantities that soluble protein can be derived in the extracellular matrix in amounts that have neuronal effects. The amount of soluble Sema7a required for neuronal action likely is much lower than the amount present physiologically as membrane-bound protein. Additional investigations are needed to determine the role of bound and soluble Sema7a during nerve regeneration as well as determine the proteases that regulate Sema7a cleavage in the cornea.

In conclusion, accumulating data support the hypothesis that nerve regeneration and inflammatory processes are linked in the cornea. Our data suggested that Sema7a influences both of these processes. However, it is unknown whether Sema7a function is normal in neurotrophic corneas, and also whether Sema7a, its derivative peptides, or strategies that enhance corneal Sema7a have therapeutic potential in treating neurotrophic keratitis.

Acknowledgments

Ke Ma, PhD, and Matthew W. Curtis, PhD, provided technical help with confocal microscopy.

References

1. Benowitz LI, Popovich PG. Inflammation and axon regeneration. *Curr Opin Neurol*. 2011;24:577–583.
2. Li Z, Burns AR, Han L, Rumbaut RE, Smith CW. IL-17 and VEGF are necessary for efficient corneal nerve regeneration. *Am J Pathol*. 2011;178:1106–1116.
3. Cruzat A, Witkin D, Baniasadi N, et al. Inflammation and the nervous system: the connection in the cornea in patients with infectious keratitis. *Invest Ophthalmol Vis Sci*. 2011;52:5136–5143.
4. Namavari A, Chaudhary, S Chang JH, et al. Cyclosporine immunomodulation retards regeneration of surgically transected corneal nerves. *Invest Ophthalmol Vis Sci*. 2012;53:732–740.
5. Sarkar J, Chaudhary S, Namavari A, et al. Corneal neurotoxicity due to topical benzalkonium chloride. *Invest Ophthalmol Vis Sci*. 2012;53:1792–1802.
6. Namavari A, Chaudhary S, Sarkar J, et al. In vivo serial imaging of regenerating corneal nerves after surgical transection in transgenic *thy1*-YFP mice. *Invest Ophthalmol Vis Sci*. 2011;52:8025–8032.
7. Chaudhary S, Namavari A, Yco L, et al. Neurotrophins and nerve regeneration-associated genes are expressed in the cornea after lamellar flap surgery [published online ahead of print June 5, 2012]. *Cornea*. 2012.
8. Okuno T, Nakatsuji Y, Kumanogoh A. The role of immune semaphorins in multiple sclerosis. *FEBS Lett*. 2011;585:3829–3835.
9. Pasterkamp RJ, Peschon JJ, Spriggs MK, Kolodkin AL. Semaphorin 7A promotes axon outgrowth through integrins and MAPKs. *Nature*. 2003;424:398–405.
10. Suzuki K, Okuno T, Yamamoto M, et al. Semaphorin 7A initiates T-cell-mediated inflammatory responses through alpha1beta1 integrin. *Nature*. 2007;446:680–684.
11. Ghanem RC, Han KY, Rojas J, et al. Semaphorin 7A promotes angiogenesis in an experimental corneal neovascularization model. *Curr Eye Res*. 2011;36:989–996.
12. Kenyon BM, Voest EE, Chen CC, Flynn E, Folkman J, D'Amato RJ. A model of angiogenesis in the mouse cornea. *Invest Ophthalmol Vis Sci*. 1996;37:1625–1632.
13. Beales MP, Funderburgh JL, Jester JV, Hassell JR. Proteoglycan synthesis by bovine keratocytes and corneal fibroblasts: maintenance of the keratocyte phenotype in culture. *Invest Ophthalmol Vis Sci*. 1999;40:1658–1663.

14. Remtulla S, Hallett PE. A schematic eye for the mouse, and comparisons with the rat. *Vision Res*. 1985;25:21–31.
15. Henriksson JT, McDermott AM, Bergmanson JP. Dimensions and morphology of the cornea in three strains of mice. *Invest Ophthalmol Vis Sci*. 2009;50:3648–3654.
16. Takamatsu H, Kumanogoh A. Diverse roles for semaphorin-plexin signaling in the immune system. *Trends Immunol*. 2012;33:127–135.
17. Okuno T, Nakatsuji Y, Kumanogoh A. The role of immune semaphorins in multiple sclerosis. *FEBS Lett*. 2011;585:3829–3835.
18. Holmes S, Downs AM, Fosberry A, et al. Sema7a is a potent monocyte stimulator. *Scand J Immunol*. 2002;56:270–275.
19. Feng G, Mellor RH, Bernstein M, et al. Imaging neuronal subsets in transgenic mice expressing multiple spectral variants of GFP. *Neuron*. 2000;28:41–51.
20. Yan Y, Sun HH, Mackinnon SE, Johnson PJ. Evaluation of peripheral nerve regeneration via in vivo serial transcutaneous imaging using transgenic Thy1-YFP mice. *Exp Neurol*. 2011;232:7–14.
21. Pan YA, Misgeld T, Lichtman JW, Sanes JR. Effects of neurotoxic and neuroprotective agents on peripheral nerve regeneration assayed by time-lapse imaging in vivo. *J Neurosci*. 2003;23:11479–11488.
22. Unezaki S, Yoshii S, Mabuchi T, Saito A, Ito S. Effects of neurotrophic factors on nerve regeneration monitored by in vivo imaging in thy1-YFP transgenic mice. *J Neurosci Methods*. 2009;178:308–315.
23. Greer JE, McGinn MJ, Povlishock JT. Diffuse traumatic axonal injury in the mouse induces atrophy, c-Jun activation, and axonal outgrowth in the axotomized neuronal population. *J Neurosci*. 2011;31:5089–5105.
24. Leung CK, Weinreb RN, Li ZW, et al. Long-term in vivo imaging and measurement of dendritic shrinkage of retinal ganglion cells. *Invest Ophthalmol Vis Sci*. 2011;52:1539–1547.
25. Yu CQ, Rosenblatt MI. Transgenic corneal neurofluorescence in mice: a new model for in vivo investigation of nerve structure and regeneration. *Invest Ophthalmol Vis Sci*. 2007;48:1535–1542.
26. Tong S, Yuan F. Dose response of angiogenesis to basic fibroblast growth factor in rat corneal pocket assay: I. Experimental characterizations. *Microvasc Res*. 2008;75:10–15.
27. Tong S, Yuan F. Dose response of angiogenesis to basic fibroblast growth factor in rat corneal pocket assay: II. Numerical simulations. *Microvasc Res*. 2008;75:16–24.
28. Andreasen SØ, Thomsen AR, Koteliansky VE, et al. Expression and functional importance of collagen-binding integrins, alpha 1 beta 1 and alpha 2 beta 1, on virus-activated T cells. *J Immunol*. 2003;171:2804–2811.
29. Kamata M, Tada Y, Uratsuji H, et al. Semaphorin 7A on keratinocytes induces interleukin-8 production by monocytes. *J Dermatol Sci*. 2011;62:176–182.
30. Bonini S, Rama P, Olzi D, Lambiase A. Neurotrophic keratitis. *Eye*. 2003;17:989–995.
31. Dastjerdi MH, Dana R. Corneal nerve alterations in dry eye-associated ocular surface disease. *Int Ophthalmol Clin*. 2009;49:11–20.
32. Wilson SE. Laser in situ keratomileusis-induced (presumed) neurotrophic epitheliopathy. *Ophthalmology*. 2001;108:1082–1087.
33. He J, Bazan HE. Omega-3 fatty acids in dry eye and corneal nerve regeneration after refractive surgery. *Prostaglandins Leukot Essent Fatty Acids*. 2010;82:319–325.
34. You L, Kruse FE, Völcker HE. Neurotrophic factors in the human cornea. *Invest Ophthalmol Vis Sci*. 2000;41:692–702.
35. Qi H, Chuang EY, Yoon KC, et al. Patterned expression of neurotrophic factors and receptors in human limbal and corneal regions. *Mol Vis*. 2007;13:1934–1941.
36. Esquenazi S, Bazan HE, Bui V, He J, Kim DB, Bazan NG. Topical combination of NGF and DHA increases rabbit corneal nerve regeneration after photorefractive keratectomy. *Invest Ophthalmol Vis Sci*. 2005;46:3121–3127.
37. Bierl MA, Jones EE, Crutcher KA, Isaacson LG. 'Mature' nerve growth factor is a minor species in most peripheral tissues. *Neurosci Lett*. 2005;380:133–137.
38. Henningsen J, Rigbolt KT, Blagoev B, Pedersen BK, Kratchmarova I. Dynamics of the skeletal muscle secretome during myoblast differentiation. *Mol Cell Proteomics*. 2010;9:2482–2496.
39. Fong KP, Barry C, Tran AN, et al. Deciphering the human platelet sheddome. *Blood*. 2011;117:e15–e26.
40. Dean RA, Overall CM. Proteomics discovery of metalloproteinase substrates in the cellular context by iTRAQ labeling reveals a diverse MMP-2 substrate degradome. *Mol Cell Proteomics*. 2007;6:611–623.
41. Ohsawa S, Hamada S, Asou H, et al. Caspase-9 activation revealed by semaphorin 7A cleavage is independent of apoptosis in the aged olfactory bulb. *J Neurosci*. 2009;29:11385–11392.
42. Azar DT, Hahn TW, Jain S, Yeh YC, Stetler-Stevensen WG. Matrix metalloproteinases are expressed during wound healing after excimer laser keratectomy. *Cornea*. 1996;15:18–24.
43. Kurpakus-Wheater M, Sexton R, McDermott ML, Mrock LK, Sosne G. Caspase-9 activation in hypoxic human corneal epithelial cells. *Apoptosis*. 2003;8:681–688.
44. Esselens C, Malapeira J, Colomé N, et al. The cleavage of semaphorin 3C induced by ADAMTS1 promotes cell migration. *J Biol Chem*. 2010;285:2463–2473.
45. Maruyama T, Matsuura M, Suzuki K, Yamamoto N. Cooperative activity of multiple upper layer proteins for thalamocortical axon growth. *Dev Neurobiol*. 2008;68:317–331.